

Reduced surface spin disorder in ZrO₂ coated γ -Fe₂O₃ nanoparticles

F. Zeb^a, M. Shoaib Khan^a, K. Nadeem^{a,*}, M. Kamran^a, H. Abbas^a, H. Krenn^b, D.V. Szabo^{c,d}

^a Nanoscience and Technology Laboratory, International Islamic University, Islamabad 44000, Pakistan

^b Institute of Physics, Karl-Franzens University, Universitätsplatz 5, A-8010 Graz, Austria

^c Institute for Applied Materials, Karlsruhe Institute of Technology (KIT), D-76344 Eggenstein-Leopoldshafen, Germany

^d Karlsruhe Nano Micro Facility (KNMF), Karlsruhe Institute of Technology (KIT), D-76344 Eggenstein-Leopoldshafen, Germany

ARTICLE INFO

Handling Editor: S. Miyashita

Keywords:

Nanoparticles

Maghemite

Zirconium dioxide

Interparticle interactions

ABSTRACT

Surface spin disorder in microwave plasma synthesized zirconium dioxide (ZrO₂) coated maghemite (γ -Fe₂O₃) nanoparticles have been studied by using AC and DC magnetic measurements. The inverse spinel structure of γ -Fe₂O₃ was confirmed by X-ray diffraction. The calculated average crystallite size of γ -Fe₂O₃ and ZrO₂ phase was about 13 and 6 nm, respectively. Zero field cooled/field cooled measurements revealed average blocking temperature at 65 K. The fitted value of K_{eff} deduced from simulation was higher than that of bulk γ -Fe₂O₃ magneto-crystalline anisotropy which is mainly due to surface spin disorder. However, it was lower than the reported value for uncoated γ -Fe₂O₃ nanoparticles, which is due to reduction in surface effects and interparticle interactions in ZrO₂ coated nanoparticles. Below 25 K, a sharp increase in saturation magnetization was observed which is due to extra contribution of frozen surface spins to magnetism at low temperatures. The coercivity also showed a sharp increase below 25 K, which is due to presence of strong core-surface interactions at low temperatures. For AC susceptibility, Arrhenius law fit revealed weak interactions among the nanoparticles which were not strong enough to create a spin-glass state. In summary, ZrO₂ coated γ -Fe₂O₃ nanoparticles showed reduced surface spin disorder and weak interparticle interactions which is due to non-magnetic ZrO₂ coating.

1. Introduction

Magnetic nanoparticles exhibit different magnetic properties as compared to their bulk materials which depend upon the size, shape and preparation technique/chemistry of the materials [1]. In fine magnetic nanoparticles, large surface to volume ratio creates disordered surface spins, which alter their magnetic properties. The surface spin disorder arises due to broken super exchange interactions at the nanoparticle's surface that produces magnetic disorder and exchange frustration at the nanoparticle's surface. The nanoparticle's surface with deficient oxygen also leads to the broken exchange bonds [2] that can produce a spin glass like state with high anisotropy [3–5]. A spin glass is a magnetically disordered state which exhibits high magnetic frustration in which each electron/atom spin freezes in a random direction below a spin glass freezing temperature [6,7].

Among different oxides of iron, maghemite (γ -Fe₂O₃) is one of the most important oxide due to its diverse and remarkable properties like high Curie temperature, non toxicity, and chemical stability which makes it promising candidate for many applications such as in ferro fluids, biomedical, data storage, and magnetic tunneling barrier [8,9]. At nano scale, the existence of surface spin disorder caused by finite size

effects usually influences the physical properties of the γ -Fe₂O₃ nanoparticles. Millan et al. [10] reported decreased magnetization in uncoated γ -Fe₂O₃ nanoparticles due to the presence of magnetically disordered surface layer. Parker et al. [11] observed a spin glass state in uncoated γ -Fe₂O₃ nanoparticles and attributed it to the strong interparticle interactions. Martinez et al. [12] also reported spin glass behavior in γ -Fe₂O₃ nanoparticles at low temperatures and attributed it to pinning effect of the frozen spins at the nanoparticle's surface.

Uncoated γ -Fe₂O₃ nanoparticles usually show agglomeration which is the effect of accumulative forces among the nanoparticles [13]. Therefore, certain specific surface protection strategies are needed to attain the stability of these nanoparticles by using suitable surface coating with specific materials either by polymers, magnetic or non magnetic material. Non magnetic coating can reduce/enhance the magnetization or spin glass behavior and avoid agglomeration of nanoparticles [14]. Therefore, it is important to coat the nanoparticles with suitable material to minimize the surface energy of the nanoparticles and weaken the strength of interactions among nanoparticles. Novotná et al. [15] prepared oleic acid coated γ -Fe₂O₃ nanoparticles and reported that oleic acid reduces the interparticle magnetic interactions. Girija et al. [16] proposed that ZrO₂ coating not only protects

* Corresponding author.

E-mail address: kashif.nadeem@iiu.edu.pk (K. Nadeem).

the magnetic nanoparticles from possible oxidation in surrounding environment but also reduces the interparticle dipolar interactions.

In this article, we have chosen a non magnetic material zirconium dioxide (ZrO_2) for coating because it has interesting properties including low toxicity and high thermal stability. It also acts as a good insulating material that can reduced the agglomeration of nano particles. It can exist in three phases which are strongly temperature dependent, these phases are monoclinic, cubic and tetragonal [17–19]. Our prime emphasis was to study the surface spin disorder in ZrO_2 coated $\gamma-Fe_2O_3$ nanoparticles by using AC and DC magnetization measurements.

2. Experimental

Microwave plasma synthesis technique has been used to synthesized ZrO_2 coated $\gamma-Fe_2O_3$ nanoparticles. The complete synthesis process is explained elsewhere [20]. Structural analysis of ZrO_2 coated $\gamma-Fe_2O_3$ nanoparticles was studied by using X ray powder diffraction (XRD) done by Bruker D8 Advance instrument by using $Cu-K\alpha$ ($\lambda = 0.154\text{ nm}$) radiation. Transmission electron microscopy (TEM) was used for the imaging of nanoparticles. Magnetic measurements (AC and DC) were done by using superconducting quantum in interface device (SQUID from Quantum Design, MPMS XL 7) magnetometry. The percentage of non magnetic ZrO_2 and magnetic $\gamma-Fe_2O_3$ phase was calculated from XRD relative intensities, and the contribution of ZrO_2 phase was subtracted from all the magnetization measurements.

3. Results and discussion

X ray diffraction (XRD) is an important technique for finding the phase and average crystallite size of the nanoparticles. Fig. 1 (a) shows the XRD scan of ZrO_2 coated $\gamma-Fe_2O_3$ nanoparticles. We have used aluminum substrate for XRD measurement. The XRD peaks at (111), (220), (311), (511) and (440) correspond to $\gamma-Fe_2O_3$ nanoparticles

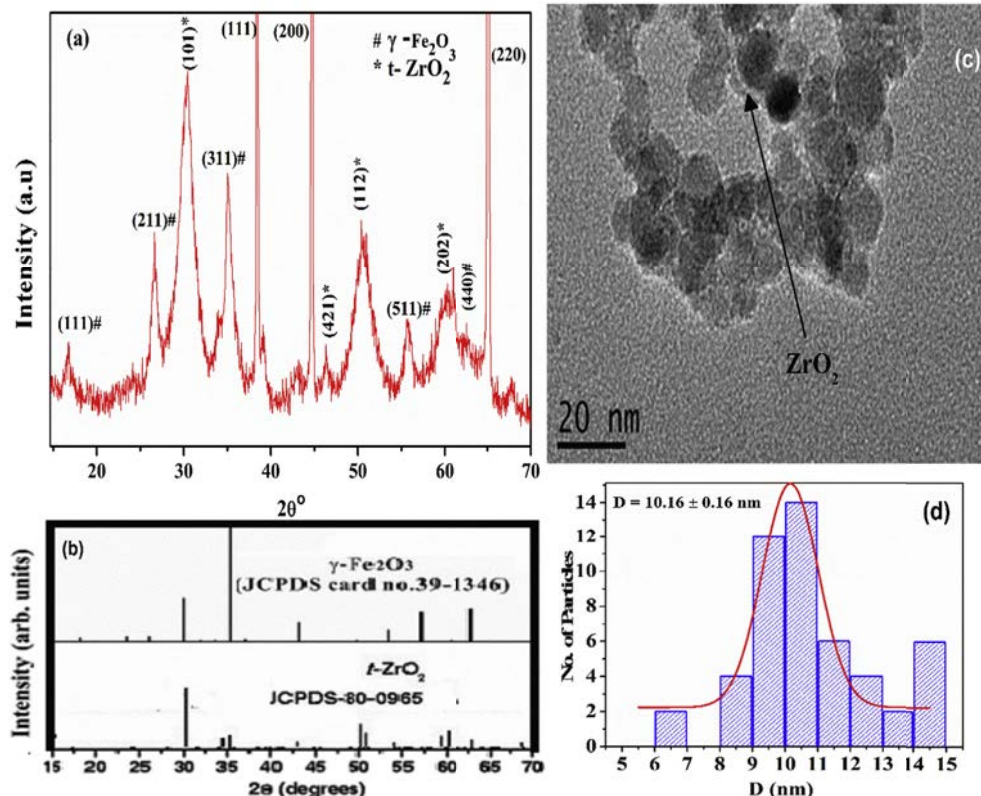


Fig. 1. (a) XRD scan of ZrO_2 coated $\gamma-Fe_2O_3$ nanoparticles, (b) JCPDS cards for $\gamma-Fe_2O_3$ and ZrO_2 , (c) TEM image of ZrO_2 coated $\gamma-Fe_2O_3$ nanoparticles at 20 nm scale and (d) particle size distribution from TEM images fitted with Gaussian distribution (red line). (For interpretation of the references to colour in this figure legend, the reader is referred to the Web version of this article.)

phase as confirmed by JCPDS card # 39 1346. A peak at 26.1° (211) is observed which is referred to magnetite [21]. The XRD peaks at (101), (100), (112) and (202) shows the presence of $t-ZrO_2$ phase [22] as confirmed by JCPDS card # 80 0965. The miller indices (111), (200) and (220) correspond to the out of scale peaks at angles 38.5° , 45° and 65° , respectively are specific for aluminum substrate. The percentage of $\gamma-Fe_2O_3$ and ZrO_2 phase has been estimated by XRD relative intensities, which comes out 32 and 68% for $\gamma-Fe_2O_3$ and ZrO_2 , respectively. The average crystallite size was about 13 and 6 nm for $\gamma-Fe_2O_3$ and ZrO_2 phases, respectively as calculated by using Debye Scherrer's formula as given below,

$$D = \frac{0.9 \lambda}{\beta \cos \theta} \quad (1)$$

Transmission electron microscopy (TEM) is a useful technique to study of shape and size of the nanoparticles. TEM image of ZrO_2 coated $\gamma-Fe_2O_3$ nanoparticles at the scale of 20 nm is shown in Fig. 1 (c). It shows that the nanoparticles are nearly spherical and less agglomerated. The particle size distribution is calculated from TEM images by using a software ImagJ and fitted with Gaussian distribution function as illustrated in Fig. 1 (d). The best fit of Gaussian best fit gives the average particle size of about $10.16 \pm 0.16\text{ nm}$.

Fig. 2 shows the experimental and simulated temperature dependent zero-field-cooled (ZFC)/field-cooled (FC) dc magnetization curves under the applied field of 50 Oe.

For measuring ZFC curve, the sample is ZFC to 5 K in zero applied field and then magnetization is measured on increasing temperature after an application of 50 Oe magnetic field. For FC curve, the sample is field cooled from 300 K under the same applied field and magnetization is measured on decreasing temperature. The ZFC curve shows a maximum around 65 K, which is the average blocking temperature (T_B) of the nanoparticles. The magnetic nanoparticles become thermally unstable for $T > T_B$ and show superparamagnetic behavior [23]. We have done simulation of ZFC/FC curves by adopting a Néel Brown relaxation model of uniaxial anisotropy. The log normal distribution function $f(V)$

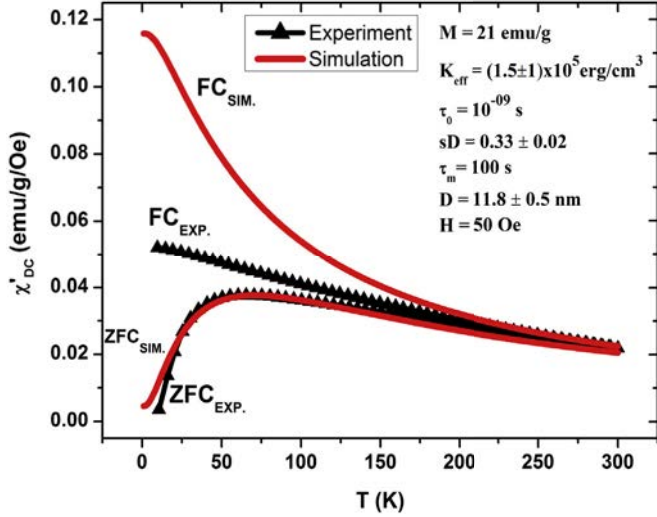


Fig. 2. Black solid up triangles represent the experimental data, while red solid lines are the simulated ZFC/FC curves of ZrO₂ coated γ -Fe₂O₃ nanoparticles. (For interpretation of the references to colour in this figure legend, the reader is referred to the Web version of this article.)

is used for the volume distribution and translated to the corresponding $f(T_B)$ for blocking temperatures T_B and is given by,

$$f(T_B)dT_B = \frac{1}{\sqrt{2\pi\sigma_{T_B}^2}} \frac{1}{T_B} \exp\left(-\frac{\ln^2 \frac{T_B}{\langle T_B \rangle}}{2\sigma_{T_B}^2}\right) dT_B \quad (2)$$

Where $\langle T_B \rangle$ is an average blocking temperature, and σ_{T_B} is the broadening (standard deviation) of the T_B distribution. The relationship between V and T_B is $K \cdot V = \ln(\tau_m/\tau_0) k_B T_B \approx 25k_B T_B$.

The ZFC/FC curves taken by a SQUID magnetometer rely on the characteristics measuring time (per temperature step) $\tau_m = 100$ s in relation with the atomic spin precession time $\tau_0 = 10^{-9} - 10^{-12}$ s.

By using Neel Brown relaxation model, the ZFC susceptibility can be written as [24],

$$\chi_{ZFC}(T) = \frac{M_S^2}{3K_{eff}} \left[\ln\left(\frac{\tau_m}{\tau_0}\right) \int_0^T \frac{T_B}{T} f(T_B) dT_B + \int_T^\infty f(T_B) dT_B \right] \quad (3)$$

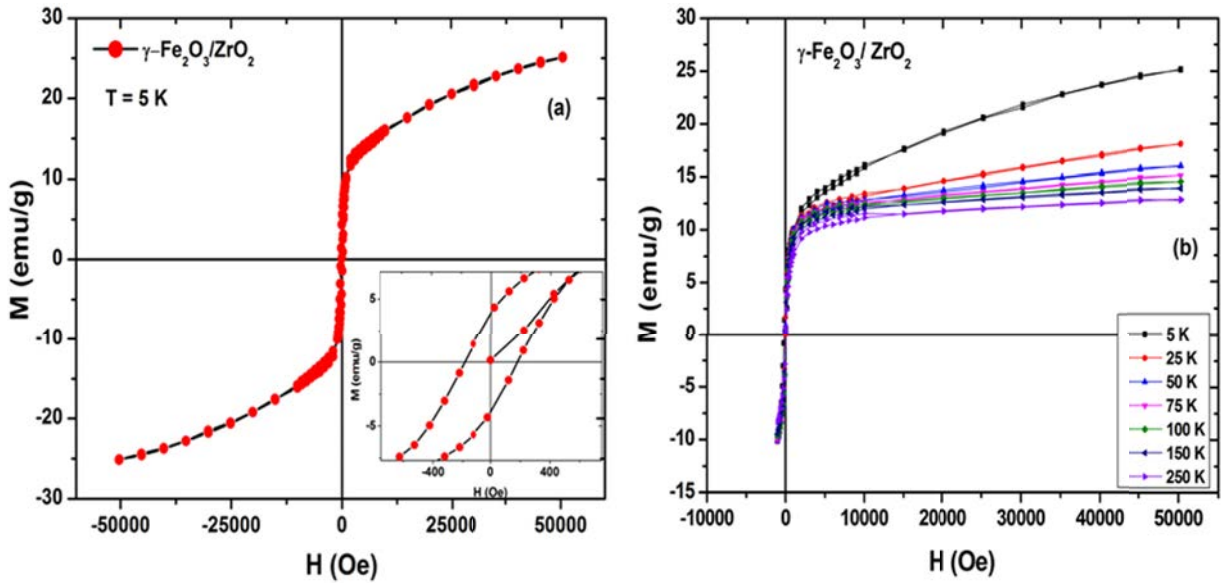


Fig. 3. (a) M-H loop at 5 K with an inset which shows the H_c region and (b) M-H partial loops of ZrO₂ coated γ -Fe₂O₃ nanoparticles at different temperatures.

For a particular temperature “T”, the first and the second term correspond to unblocked superparamagnetic and blocked particles, respectively.

FC susceptibility is given by the same model is [24],

$$\chi_{FC}(T) = \frac{M_S^2}{3K_{eff}} \ln\left(\frac{\tau_m}{\tau_0}\right) \left[\frac{1}{T} \int_0^T T_B f(T_B) dT_B + \int_T^\infty f(T_B) dT_B \right] \quad (4)$$

The simulated ZFC/FC curves showed that the values obtained for effective anisotropy constant (K_{eff}) and average particle size are $(1.5 \pm 1) \times 10^5$ erg/cm³ and 11.8 ± 0.5 nm, respectively. The higher value of simulated K_{eff} as compared to bulk γ -Fe₂O₃ ($K_{bulk} = 4.7 \times 10^4$ erg/cm³) [25] is due to the fact that the model does not take into account the surface anisotropy: $K_{eff} = K_{bulk} + K_{surface}/\langle d \rangle$. The average crystallite size as obtained from simulated curve is in agreement with the TEM analysis [26]. Uncoated bare γ -Fe₂O₃ nanoparticles as prepared by the same method were reported with enhanced K_{eff} value (9.8×10^5 erg/cm³) [27]. Here ZrO₂ coating affects the K_{eff} but is smaller than the K_{eff} of bare γ -Fe₂O₃ nanoparticles prepared by same method [27], which is attributed to weak dipolar interactions and surface effects in ZrO₂ coated γ -Fe₂O₃ nanoparticles. The experimental FC curve becomes flattened just below T_B , which is mainly due to the presence of interparticle interactions [28]. The discrepancy in the experimental and simulated FC curves is due to the fact that model considers only non interacting particles.

Fig. 3 (a) and (b) shows the M-H loop at 5 K and M-H partial loops at different temperatures ranging from 5 to 250 K, respectively.

It is evident that M-H loops are not completely saturated even at 5 T, which is due to presence of disordered frozen surface spins. Here the frozen and random/disordered surface spins exhibit strong interactions with each other i.e. core and surface spins. At 5 K, the higher value of coercivity (H_c) is related to the onset of surface magnetic anisotropy caused by frozen disordered surface spins. Fig. 3(a) shows that M_s has maximum value of about 25.1 emu/g (after subtraction of mass percentage (g) of non magnetic ZrO₂ phase) at 5 T, which is less than the bulk value of γ -Fe₂O₃ (80 emu/g) and is mainly due to disordered surface spin structure originated from size reduction [29,30]. Kodama et al. [31] presented a computational model on disordered spin freezing at the surface of ferrite nanoparticles and they reported that randomly arranged spins are responsible in M_s reduction [32]. Such a decrease in M_s value with decreasing nanoparticle's size is typical for ferrite nanoparticles and is attributed to disordered surface spins [33].

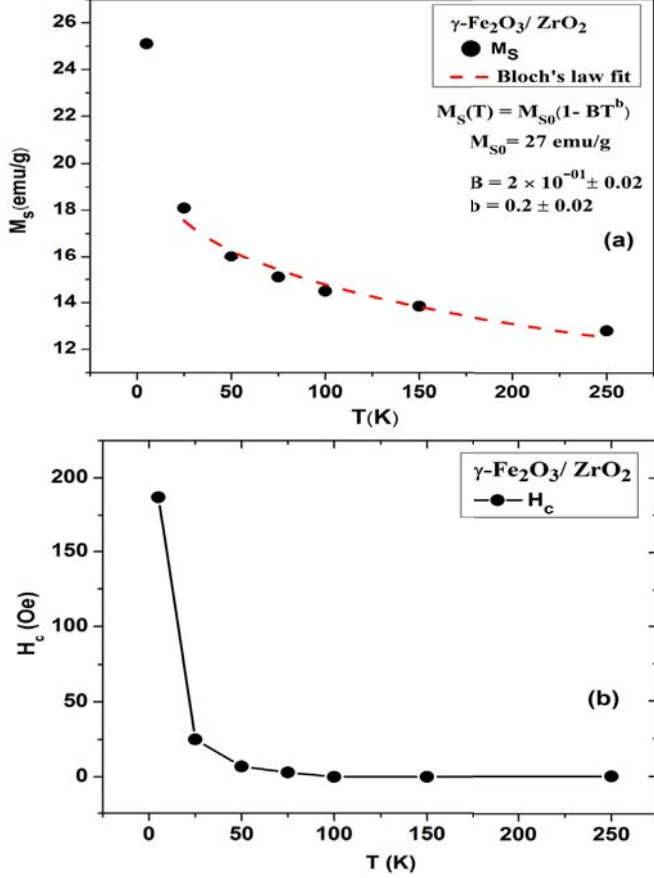


Fig. 4. (a) Variation of saturation magnetization for ZrO₂ coated γ -Fe₂O₃ nanoparticles with “Bloch's law” fit (red dashed line), and (b) variation of coercivity for ZrO₂ coated γ -Fe₂O₃ nanoparticles. (For interpretation of the references to colour in this figure legend, the reader is referred to the Web version of this article.)

Fig. 4 (a) shows the temperature dependent saturation magnetization (M_s) ranging from 5 to 250 K. For saturating ferromagnetic/ferromagnetic materials below T_c , M_s follows the Bloch's law [34] as given below,

$$M_s(T) = M_s(0)(1 - BT^b) \quad (5)$$

Where $M_s(T)$, $M_s(0)$, B and b represents the temperature dependent saturation magnetization, spontaneous magnetization obtained by extra plotting to 0 K, Bloch's constant and the Bloch's exponent, respectively. The Bloch's law is usually effective for ferromagnetic/ferrimagnetic bulk materials, in which excitation of spin waves are responsible for temperature dependent magnetization [34–36].

It is observed that the M_s increases sharply below 25 K. In fact, ZrO₂ coating eases the alignment of core shell and surface spins with an external magnetic field at low temperatures especially at 5 K [37]. This kind of sharp increase in M_s is not reported for bare γ -Fe₂O₃ nanoparticles prepared by the same method [28]. The increase in M_s suggests the reduction in surface effects in these nanoparticles, which is probably due to non magnetic ZrO₂ coating. Bloch's law fails to fit at lower temperatures due to sharp increase in M_s value. The fit gives a Bloch's exponent value $b = 0.2 \pm 0.02$ which is much lower than the bulk value ($b = 1.5$). Fig. 4 (b) shows the variation of coercivity (H_c) with temperature for ZrO₂ coated γ -Fe₂O₃ nanoparticles. The H_c also shows a sharp pronounced increase below 25 K, which is attributed to the strong surface anisotropy contribution of the disordered frozen surface spins because surface spins get blocked at rather low temperatures than huge nanoparticle's core spin. Therefore strong surface anisotropy and surface structural inhomogeneity affect the coercivity of

ferrite nanoparticles. The Kneller's law was used to fit the H_c vs T data but it completely failed due to a sharp increase of H_c below 25 K [38].

For the investigation of dynamics response of the nanoparticles, AC susceptibility measurements were taken at different frequencies. These measurements give us information about the phase transitions in ordered state, spin reorientation/metamagnetic transitions, change in anisotropy energy and magnetic state of blocked nanoparticles in dependence of the varying frequency dependent measuring time $\tau_m = 1/f$. Fig. 5 (a) and (b) shows the temperature dependent in phase and out of phase AC susceptibility, respectively for ZrO₂ coated γ -Fe₂O₃ nanoparticles at different frequencies (f) = 1, 10, 100, and 1000 Hz.

The in phase AC susceptibility shows an increase in T_B from 77 K to 102 K with varying frequency from 1 to 1000 Hz. Interparticle interactions and surface spin disorder are mainly responsible for such a small variation in T_B with increasing frequency. The frequency shift of T_B can be due to superparamagnetic, spin glass state and interparticle interactions in these nanoparticles [39]. The out of phase part of AC susceptibility also shows a small variation in T_B with frequency as shown in Fig. 5(b). The f shift of T_B is further investigated by an Arrhenius law as shown in Fig. 5 (c). The Arrhenius law is valid for non interacting monodispersed nanoparticles having uniaxial anisotropy energy barrier, given as [40]

$$\tau_m = \tau_0 \exp\left(\frac{E_a}{k_B T_B}\right) \quad (6)$$

Where τ_m is the measuring spin flip time, τ_0 is the atomic spin flip time ranges from 10^{-9} to 10^{-12} s, E_a indicates the anisotropy energy and $k_B T_B$ is the thermal energy [37,41]. From Arrhenius law fit, we deduced the values for activation energy and atomic spin flip time which are 2228 ± 256 K and $3 \times 10^{-13} \pm 10^{-01}$ s, respectively. It shows that these ZrO₂ coated nanoparticles do not completely follow thermally activated Arrhenius law but a slight lower value of τ_0 ensures the existence of weak interparticle interactions in these nanoparticles [42–44].

4. Conclusions

The crystalline ZrO₂ and γ -Fe₂O₃ phases were confirmed by the XRD analysis. Temperature dependent ZFC/FC curves revealed T_B of the nanoparticles at 65 K under an applied field of 50 Oe. The simulation of ZFC/FC curves revealed a higher value of K_{eff} as compared to bulk γ -Fe₂O₃ but lower than the reported uncoated γ -Fe₂O₃ nanoparticles prepared by the same method. It ensures the existence of surface spin disorder in these ZrO₂ coated nanoparticles but is weaker than in the uncoated maghemite nanoparticles and it is attributed to the ZrO₂ coating. Saturation magnetization revealed a lower value (25.1 emu/g) as compared to that of bulk value (80 emu/g), which is attributed to disordered surface spins. The sharp increased value of M_s below 25 K is due to reduced surface spin disorder in these nanoparticles. A sharp increase in H_c below 25 K is mainly due to the existence of strong core shell interactions. The Arrhenius law fitting reveals a value of spin flip time (τ_0) = 3×10^{-13} s, which is near to atomic spin flip time (10^{-9} to 10^{-12} s) and is attributed to weak interparticle interactions. The main influence of ZrO₂ coating on γ -Fe₂O₃ nanoparticles is to reduce the surface spin disorder and interparticle interactions as compared to uncoated γ -Fe₂O₃ nanoparticles. In conclusion, ZrO₂ surface coating can be beneficial in controlling the magnetism of soft magnetic nanoparticles and stabilizing the nano magnetic blocking behavior by avoiding agglomeration for diverse applications.

Acknowledgments

K. Nadeem acknowledges Higher Education Commission (HEC) of Pakistan for financial support. Authors also acknowledge International Islamic University, Islamabad for providing research funds under

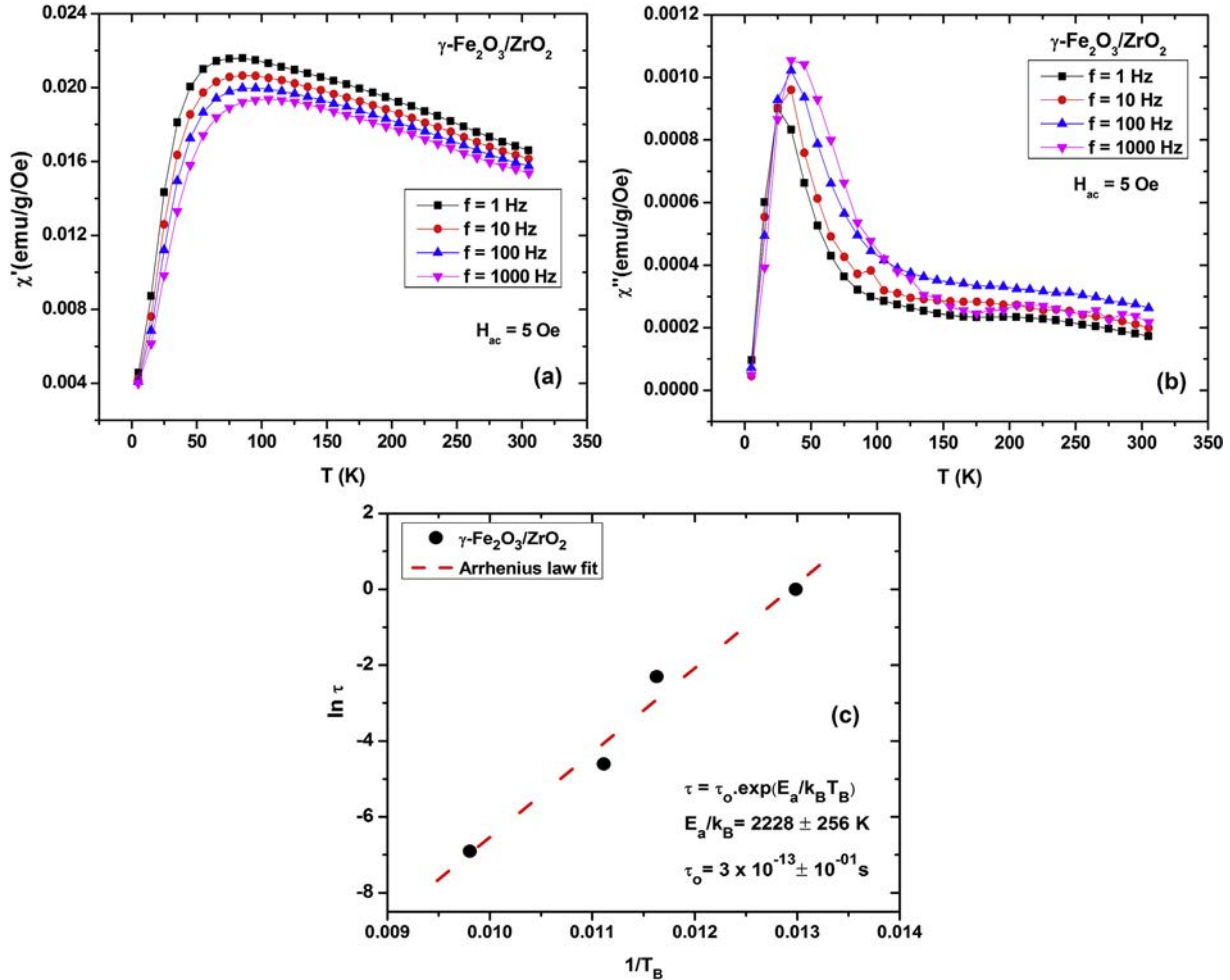


Fig. 5. (a) and (b) are in-phase and out-of-phase AC susceptibility at different frequencies, respectively and (c) Arrhenius law fit for ZrO₂ coated γ -Fe₂O₃ nanoparticles.

References

- [1] S. Ayyappan, S. Mahadevan, P. Chandramohan, M. Srinivasan, J. Philip, B. Raj, Influence of Co²⁺ ion concentration on the size, magnetic properties, and purity of CoFe₂O₄ spinel ferrite nanoparticles, *J. Phys. Chem. C* 114 (2010) 6334–6341.
- [2] R.H. Kodama, A.E. Berkowitz, E. McNiff Jr., S. Foner, Surface spin disorder in NiFe₂O₄ nanoparticles, *Phys. Rev. Lett.* 77 (1996) 394.
- [3] R. Kodama, Magnetic nanoparticles, *J. Magn. Magn. Mater.* 200 (1999) 359–372.
- [4] E.M. Chudnovsky, L. Gunther, Quantum tunneling of magnetization in small ferromagnetic particles, *Phys. Rev. Lett.* 60 (1988) 661.
- [5] D. Fiorani, A. Testa, F. Lucari, F. D'Orazio, H. Romero, Magnetic properties of maghemite nanoparticle systems: surface anisotropy and interparticle interaction effects, *Phys. B Condens. Matter* 320 (2002) 122–126.
- [6] V. Cannella, J. Mydosh, Magnetic ordering in gold-iron alloys, *Phys. Rev. B* 6 (1972) 4220.
- [7] S. Kirkpatrick, D. Sherrington, Infinite-ranged models of spin-glasses, *Phys. Rev. B* 17 (1978) 4384.
- [8] J.A. Wiemann, E.E. Carpenter, J. Wiggins, W. Zhou, J. Tang, S. Li, V.T. John, G.J. Long, A. Mohan, Magnetoresistance of a (γ -Fe₂O₃) 80 Ag 20 nanocomposite prepared in reverse micelles, *J. Appl. Phys.* 87 (2000) 7001–7003.
- [9] H. Yanagihara, M. Hasegawa, E. Kita, Y. Wakabayashi, H. Sawa, K. Siratori, Iron vacancy ordered γ -Fe₂O₃ (001) epitaxial films: the crystal structure and electrical resistivity, *J. Phys. Soc. Jpn.* 75 (2006) 054708.
- [10] A. Millan, A. Urtizberea, N. Silva, F. Palacio, V. Amaral, E. Snoeck, V. Serin, Surface effects in maghemite nanoparticles, *J. Magn. Magn. Mater.* 312 (2007) L5–L9.
- [11] D. Parker, V. Dupuis, F. Ladieu, J.-P. Bouchaud, E. Dubois, R. Perzynski, E. Vincent, Spin-glass behavior in an interacting γ -Fe₂O₃ nanoparticle system, *Phys. Rev. B* 77 (2008) 104428.
- [12] B. Martinez, X. Obradors, L. Balcells, A. Rouanet, C. Monty, Low temperature surface spin-glass transition in γ -Fe₂O₃ nanoparticles, *Phys. Rev. Lett.* 80 (1998) 181.
- [13] S. Laurent, D. Forge, M. Port, A. Roch, C. Robic, L. Vander Elst, R.N. Muller, Magnetic iron oxide nanoparticles: synthesis, stabilization, vectorization, physico-chemical characterizations, and biological applications, *Chem. Rev.* 108 (2008) 2064–2110.
- [14] W. Wu, Q. He, C. Jiang, Magnetic iron oxide nanoparticles: synthesis and surface functionalization strategies, *Nanoscale Res. Lett.* 3 (2008) 397–415.
- [15] V. Novotná, J. Vejpravová, V. Hamplová, J. Prokleska, E. Gorecka, D. Pocięcha, N. Podoliak, M. Glogarová, Nanocomposite of superparamagnetic maghemite nanoparticles and ferroelectric liquid crystal, *RSC Adv.* 3 (2013) 10919–10926.
- [16] G.S. Chaubey, J.-K. Kim, Structure and magnetic characterization of core-shell Fe@ZrO₂ nanoparticles synthesized by sol-gel process, *Bull. Kor. Chem. Soc.* 28 (2007) 2279–2282.
- [17] H. Tiainen, G. Eder, O. Nilsen, H.J. Haugen, Effect of ZrO₂ addition on the mechanical properties of porous TiO₂ bone scaffolds, *Mater. Sci. Eng. C* 32 (2012) 1386–1393.
- [18] H. Liu, S. Li, Q. Li, Y. Li, W. Zhou, Microstructure, phase stability and thermal conductivity of plasma sprayed Yb₂O₃, Y₂O₃ co-stabilized ZrO₂ coatings, *Solid State Sci.* 13 (2011) 513–519.
- [19] A. Ortiz, J. Sánchez-González, L. González-Méndez, F. Cumbreira, Determination of the thermal stability and isothermal bulk modulus of the ZrO₂ polymorphs at room temperature by molecular dynamics with a semi-empirical quantum-chemical model, *Ceram. Int.* 33 (2007) 705–709.
- [20] D. Vollath, D.V. Szabó, The Microwave plasma process—a versatile process to synthesize nanoparticulate materials, *J. Nanopart. Res.* 8 (2006) 417–428.
- [21] W. Kim, C.-Y. Suh, S.-W. Cho, K.-M. Roh, H. Kwon, K. Song, I.-J. Shon, A new method for the identification and quantification of magnetite–maghemite mixture using conventional X-ray diffraction technique, *Talanta* 94 (2012) 348–352.
- [22] J.D. Osorio, A. Lopera-Valle, A. Toro, J.P. Hernández-Ortiz, Phase transformations in air plasma-sprayed yttria-stabilized zirconia thermal barrier coatings, *Dyna* 81 (2014) 13–18.

- [23] M. Benitez, P. Szary, D. Mishra, M. Feyen, A. Lu, O. Petravic, H. Zabel, Templated Self-assembly of Iron Oxide Nanoparticles, arXiv preprint (2010) arXiv:1010.4166.
- [24] J. Denardin, A. Brandl, M. Knobel, P. Panissod, A. Pakhomov, H. Liu, X. Zhang, Thermoremanence and zero-field-cooled/field-cooled magnetization study of $\text{Co}_x(\text{SiO}_2)_{1-x}$ granular films, *Phys. Rev. B* 65 (2002) 064422.
- [25] E. Valstyn, J. Hanton, A. Morrish, Ferromagnetic resonance of single-domain particles, *Phys. Rev.* 128 (1962) 2078.
- [26] J.-L. Dormann, D. Fiorani, E. Tronc, Magnetic relaxation in fine-particle systems, *Adv. Chem. Phys.* 98 (2007) 283–494.
- [27] K. Nadeem, H. Krenn, T. Traußnig, R. Würschum, D. Szabó, I. Letofsky-Papst, Spin-glass freezing of maghemite nanoparticles prepared by microwave plasma synthesis, *J. Appl. Phys.* 111 (2012) 113911.
- [28] K. Nadeem, H. Krenn, T. Traussnig, R. Würschum, D. Szabó, I. Letofsky-Papst, Effect of dipolar and exchange interactions on magnetic blocking of maghemite nanoparticles, *J. Magn. Magn. Mater.* 323 (2011) 1998–2004.
- [29] Z. Shaterabadi, G. Nabiyouni, M. Soleymani, High impact of in situ dextran coating on biocompatibility, stability and magnetic properties of iron oxide nanoparticles, *Mater. Sci. Eng. C* 75 (2017) 947–956.
- [30] X. Lin, C. Sorensen, K. Klabunde, G. Hadjipanayis, Temperature dependence of morphology and magnetic properties of cobalt nanoparticles prepared by an inverse micelle technique, *Langmuir* 14 (1998) 7140–7146.
- [31] R.H. Kodama, A.E. Berkowitz, Atomic-scale magnetic modeling of oxide nanoparticles, *Phys. Rev. B* 59 (1999) 6321.
- [32] J. Smit, H.P.J. Wijn, Ferrites: Physical Properties of Ferrimagnetic Oxides in Relation to Their Technical Applications, Wiley, 1959.
- [33] C. Verdes, B. Ruiz-Diaz, S. Thompson, R. Chantrell, A. Stancu, Computational model of the magnetic and transport properties of interacting fine particles, *Phys. Rev. B* 65 (2002) 174417.
- [34] F. Bloch, Zur theorie des ferromagnetismus, *Z. Phys.* 61 (1930) 206–219.
- [35] H. Zijlstra, E. Wohlfarth, *Ferromagnetic Materials* vol. 3, North-Holland, Amsterdam, 1982.
- [36] K. Maaz, A. Mumtaz, S. Hasanain, M. Bertino, Temperature dependent coercivity and magnetization of nickel ferrite nanoparticles, *J. Magn. Magn. Mater.* 322 (2010) 2199–2202.
- [37] C. Bean, J. Livingston, Superparamagnetism, *J. Appl. Phys.* 30 (1959) S120–S129.
- [38] T. Shendruk, R. Desautels, B. Southern, J. Van Lierop, The effect of surface spin disorder on the magnetism of $\gamma\text{-Fe}_2\text{O}_3$ nanoparticle dispersions, *Nanotechnology* 18 (2007) 455704.
- [39] C. Nayek, K. Manna, G. Bhattacharjee, P. Murugavel, I. Obaidat, Investigating size- and temperature-dependent coercivity and saturation magnetization in PEG coated Fe_3O_4 nanoparticles, *Magnetochemistry* 3 (2017) 19.
- [40] J. Gonzdez, M. Montero, X. Batlle, A. Labarta, Agnetization reversal mechanisms in colloidal dispersions of magnetite particles, *IEEE Trans. Magn.* 34 (1998).
- [41] S. Shtrikman, E. Wohlfarth, The theory of the Vogel-Fulcher law of spin glasses, *Phys. Lett. A* 85 (1981) 467–470.
- [42] S.H. Masunaga, R.d.F. Jardim, P.F.P. Fichtner, J. Rivas, Role of dipolar interactions in a system of Ni nanoparticles studied by magnetic susceptibility measurements, *Phys. Rev. B* 80 (2009) 184428.
- [43] C. Cannas, G. Concas, D. Gatteschi, A. Falqui, A. Musinu, G. Piccaluga, C. Sangregorio, G. Spano, Superparamagnetic behaviour of $\gamma\text{-Fe}_2\text{O}_3$ nanoparticles dispersed in a silica matrix, *Phys. Chem. Chem. Phys.* 3 (2001) 832–838.
- [44] F. Zeb, M. Ishaque, K. Nadeem, M. Kamran, H. Krenn, D.V. Szabo, U. Brossmann, I. Letofsky-Papst, Reduced surface effects in weakly interacting ZrO_2 coated MnFe_2O_4 nanoparticles, *J. Magn. Magn. Mater.* 469 (2019) 580–586.

Repository KITopen

Dies ist ein Postprint/begutachtetes Manuskript.

Empfohlene Zitierung:

Zeb, F.; Shoaib Khan, M.; Nadeem, K.; Kamran, M.; Abbas, H.; Krenn, H.; Szabo, D. V.

[Reduced surface spin disorder in ZrO₂ coated \$\gamma\$ -Fe₂O₃ nanoparticles](#)

2018. Solid state communications, 284-286

[doi: 10.554/IR/1000086387](#)

Zitierung der Originalveröffentlichung:

Zeb, F.; Shoaib Khan, M.; Nadeem, K.; Kamran, M.; Abbas, H.; Krenn, H.; Szabo, D. V.

[Reduced surface spin disorder in ZrO₂ coated \$\gamma\$ -Fe₂O₃ nanoparticles](#)

2018. Solid state communications, 284-286, 69–74.

[doi:10.1016/j.ssc.2018.09.010](#)